Current Measurement of Digital Field Oriented Control

Seung-Ho Song, Jong-Woo Choi and Seung-Ki Sul
School of Electrical Engineering, Seoul National University, Seoul, Korea

***Abstract* - This paper studies current measurement issue of all digital field oriented control of AC motors. The paper focuses on the effect of antialiasing filter and also on the sampling of the fundamental components of the motor current. The antialiasing filter, which suppresses the high frequency component of the motor current, introduces cross coupling effects on the D and Q axis current regulation and limits the bandwidths of the current regulator because of its phase lag. In this paper a novel sampling technique is proposed to sample the fundamental component of the current without antialiasing filter. It is based on the characteristic of the symmetry pulse width modulation. With this technique, the bandwidth of current regulator can be extended to the limit given by switching frequency of the inverter and more precise torque regulation is possible.**

I. INTRODUCTION

The current regulator is an essential part of AC motor drive system. The performance of field oriented control of AC motor greatly depends on the performance of the regulator. Hence, there are many studies to improve the performance of the regulator[1~7]. Also due to the development of the high speed switching power device such as IGBT and MOSFET, the switching frequency of the inverter is gradually increasing. The hardware and software technique of digital signal processing is getting advanced and the bandwidth of the regulator is rapidly improved. Nowadays, most of the recently developed AC drive system employs all digital implementation of the control algorithms including current regulation loop. The sampling time of the current regulation loop is getting less than 100μsec.

It is well known that, to prevent aliasing effect, the highest frequency component of the input of the digital control system should be less than a half of the sampling frequency of the controller. To do that, a low pass filter is used for antialiasing. The effect of the filter in field oriented control is well described in [8]. The filter introduces D and Q axis cross coupling and gives time delay in the control loop. Ideally, the fundamental component of the motor current driven by a PWM inverter can be sampled without low pass antialiasing filter, which depends on PWM strategy. In the real implementation, the low pass filter is inevitably used not for antialiasing but for suppression of switching noise. In this paper the effect of the low pass filter is investigated and a technique to compensate the delay of the filter is proposed. Through the computer simulation and experiment the effectiveness of the proposed technique is verified.

II. EFFECT OF ANTIALIASING FILTER

Generally, to prevent aliasing phenomenon, the analog low-pass filter acting on phase currents is used. If a second order low pass filter whose natural frequency is ω_n and damping is ζ is used, the relation between real 3-phase currents and filtered 3-phase currents can be written as (1).

$$\mathbf{i}_{abcf} = \frac{\omega_n^2}{s^2 + 2\zeta\omega_n s + \omega_n^2}\mathbf{i}_{abc}. \tag{1}$$

Because the 3-phase currents must sum to zero, the relation between real d-q currents and filtered d-q currents in stationary reference frame can be easily obtained from (1).

$$\mathbf{i}^s_{dqf} = \frac{\omega_n^2}{s^2 + 2\zeta\omega_n s + \omega_n^2}\mathbf{i}^s_{dq}. \tag{2}$$

In (1) and (2), $\mathbf{i}_{abc}$ is real 3-phase current vector, $\mathbf{i}_{abcf}$ is filtered 3-phase current vector, $\mathbf{i}^s_{dq}$ is real d-q current vector and $\mathbf{i}^s_{dqf}$ is filtered d-q current vector in stationary reference frame. In this paper, the subscript '*f*' means that the variable is the output of the filter and the superscript '*s*' denotes that the variable is in the stationary reference frame. Equation (2) can also be expressed in state space form as (3).

$$\dot{\mathbf{x}} = \mathbf{A}\,\mathbf{x} + \mathbf{B}\,\mathbf{i}^s_{dq} \tag{3}$$

where

$$\mathbf{A} = \begin{bmatrix} 0 & 1 & 0 & 0 \\ -\omega_n^2 & -2\zeta\omega_n & 0 & 0 \\ 0 & 0 & 0 & 1 \\ 0 & 0 & -\omega_n^2 & -2\zeta\omega_n \end{bmatrix},$$

$$\mathbf{B} = \begin{bmatrix} 0 & 0 \\ \omega_n^2 & 0 \\ 0 & 0 \\ 0 & \omega_n^2 \end{bmatrix},$$

$$\mathbf{x} = \begin{bmatrix} i^s_{df} & \dot{i}^s_{df} & i^s_{qf} & \dot{i}^s_{qf} \end{bmatrix}^T,$$

$$\mathbf{i}^s_{dq} = \begin{bmatrix} i^s_d & i^s_q \end{bmatrix}^T.$$

In order to analyze the effects of the antialiasing filters on field oriented controller, the dynamics of the filters should be transformed into the synchronously rotating reference frame.

$$\dot{\mathbf{z}} = \mathbf{C}\,\mathbf{z} + \mathbf{D}\,\mathbf{i}_{dq}^{e} \tag{4}$$

where

$$\mathbf{C} = \begin{bmatrix} 0 & 1 & 0 & 0 \\ -\omega_n^2 + \omega_e^2 & -2\zeta\omega_n & (\frac{d\omega_e}{dt} + 2\zeta\omega_n\omega_e) & 2\omega_e \\ 0 & 0 & 0 & 1 \\ -(\frac{d\omega_e}{dt} + 2\zeta\omega_n\omega_e) & -2\omega_e & -\omega_n^2 + \omega_e^2 & -2\zeta\omega_n \end{bmatrix},$$

$$\mathbf{D} = \begin{bmatrix} 0 & 0 \\ \omega_n^2 & 0 \\ 0 & 0 \\ 0 & \omega_n^2 \end{bmatrix},$$

$$\mathbf{z} = \begin{bmatrix} i_{df}^{e} & \dot{i}_{df}^{e} & i_{qf}^{e} & \dot{i}_{qf}^{e} \end{bmatrix}^T,$$

$$\mathbf{i}_{dq}^{e} = \begin{bmatrix} i_d^e & i_q^e \end{bmatrix}^T.$$

In (4), $\mathbf{i}_{dq}^{e}$ is real d-q current vector and $\mathbf{i}_{dqf}^{e}$ is filtered d-q current vector in synchronous reference frame. In addition, the superscript 'e' denotes that the variable is in synchronous reference frame and ω_e is the electrical angular frequency of motor. Notice that even though (3) shows the perfect decoupling between i_{df}^{s} and i_{qf}^{s}, there exists the cross coupling between i_{df}^{e} and i_{qf}^{e} in the synchronously rotating reference frame. In steady state, (4) is reduced to the simple relation between $\mathbf{i}_{dq}^{e}$ and $\mathbf{i}_{dqf}^{e}$ as (5).

$$\mathbf{i}_{dq}^{e} = \begin{bmatrix} \dfrac{\omega_n^2 - \omega_e^2}{\omega_n^2} & \dfrac{-2\zeta\omega_e}{\omega_n} \\ \dfrac{2\zeta\omega_e}{\omega_n} & \dfrac{\omega_n^2 - \omega_e^2}{\omega_n^2} \end{bmatrix} \mathbf{i}_{dqf}^{e} \tag{5}$$

where

$$\mathbf{i}_{dqf}^{e} = \begin{bmatrix} i_{df}^{e} & i_{qf}^{e} \end{bmatrix}^T.$$

For example, the magnitude of steady state cross coupling is 8.8% when ω_n is $2\pi\times1600$[rad/sec], ζ is 0.707 and ω_e is $2\pi\times100$[rad/sec]. The cross coupling effect is getting severe as operating frequency is increasing and cut-off frequency of the filter is decreasing[8]. Practically, to prevent aliasing phenomenon effectively, the filter natural frequency should be less than one fifth of the sampling frequency.

Fig. 1 shows the unit step responses of the current regulator according to different bandwidth of the current regulator with the same cut-off frequency (1.6kHz) low pass filter. The parameters used in simulation and experimental

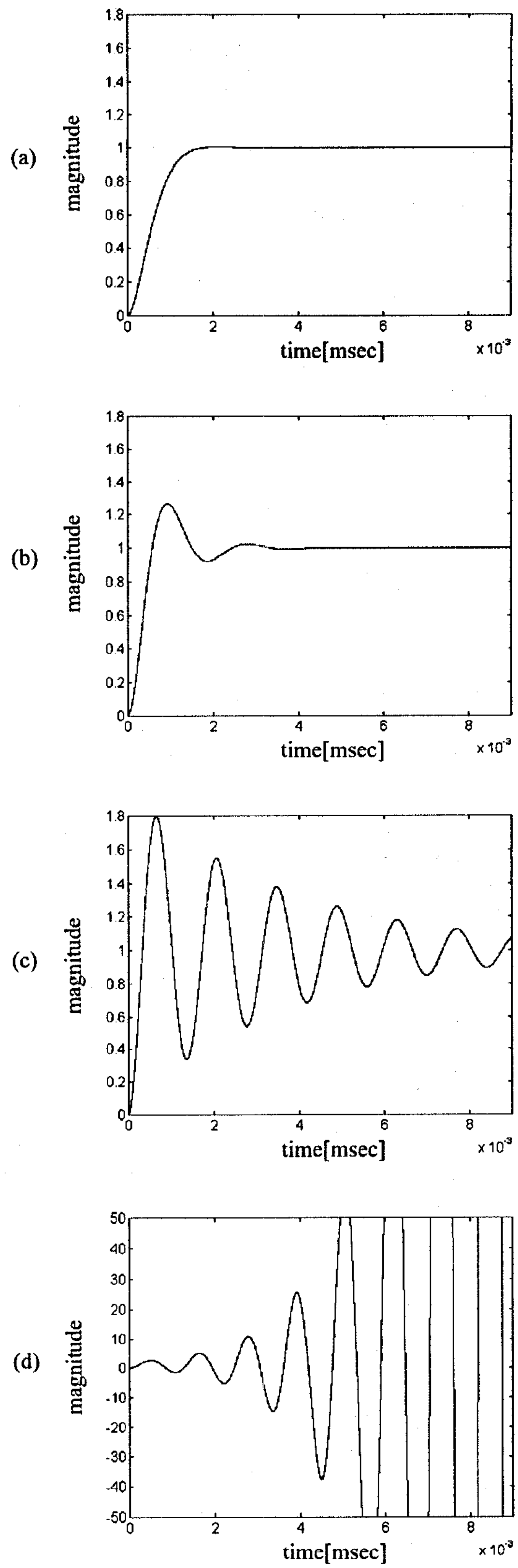

Fig. 1. Unit step responses of the current regulator according to the bandwidth of current regulator under same cut-off frequency antialiasing filter ((a) Bandwidth = 200[Hz], (b) Bandwidth = 400[Hz], (c) Bandwidth = 800[Hz], (d) Bandwidth = 1600[Hz])

study are shown in the appendix. From the figure, it can be concluded that the maximum bandwidth of the regulator is a half of the natural frequency of the filter and other special measure is needed to increase the maximum bandwidth.

III. PWM Strategy and Current Sampling

The characteristics of the harmonic frequency are determined according to each PWM strategy. In the deterministic PWM contrast to random PWM, the harmonic spectrum is clearly defined[9,10]. In case of sine triangular PWM and 3 phase symmetry space vector PWM, the lowest harmonic of the motor current is around the twice of the switching frequency. If the sampling frequency is twice of the switching frequency and it is synchronized to PWM signals, the fundamental current can be sampled without any filtering.

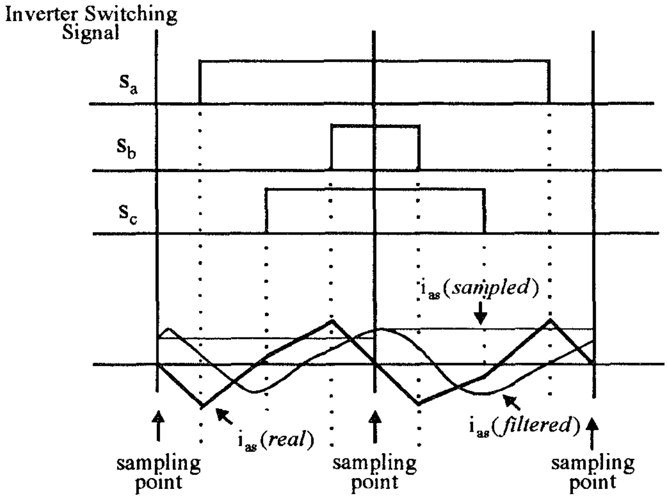

Fig. 2. PWM signals, motor current, sampling point, filtered current and sampled current at typical operating condition

Fig. 2 shows PWM signals, motor current, sampling point, filtered current and sampled current at typical operating condition. In the real implementation of the current sampling system the low pass filter to suppress the inverter switching noise is inevitable. If the current is sampled through a low pass filter, the motor current could be delayed and the sampled current is not the fundamental component. As an example, shown in Fig. 2, if the filter cut-off frequency is the same with the frequency of the sampling, the sampled current is almost the peak value of the motor current. The effect of filter at the sampling of the current results in not only the magnitude error but also phase error, which is shown in Fig. 3. The phase and magnitude error of the measured current degrades the performance of the field orientation control of the machine drive system.

This error can be avoided if the sampling is also delayed according to the delay of the filter. The simulation result for the delayed sampling is shown in Fig. 4. The delayed sampling provides almost average value of the motor current within a sampling interval. The comparison between without and with delayed sampling is given in Fig. 5. As shown in Fig. 5(b), the delayed sampling has no phase and magnitude error.

These simulation results can also be experimentally ascertained as Fig. 6 ~ Fig. 8.

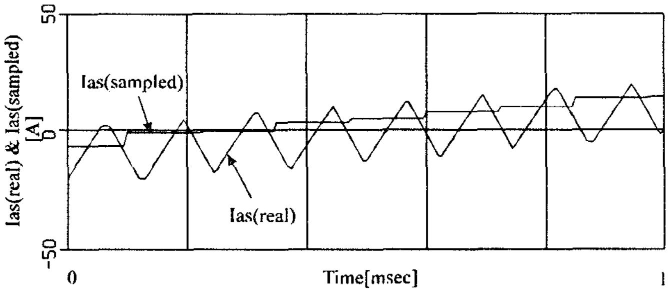

Fig. 3. Real current and sampled current without delayed sampling (simulation)

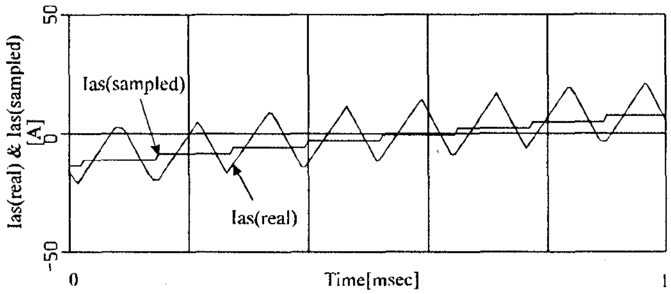

Fig. 4. Real current and sampled current with delayed sampling (simulation)

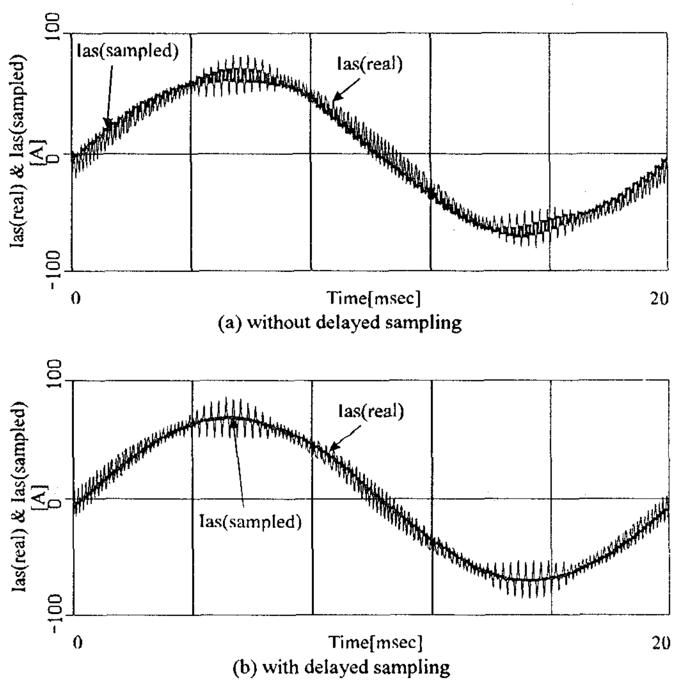

Fig. 5. Real current and sampled current without and with delayed sampling (simulation : bold line indicates sampled current)

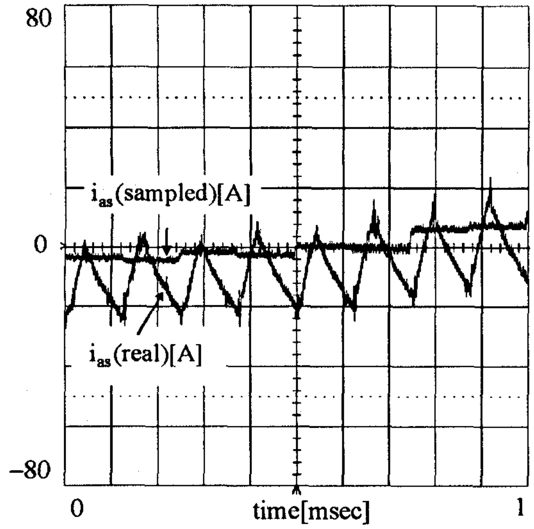

Fig. 6. Real current and sampled current without delayed sampling (experiment)

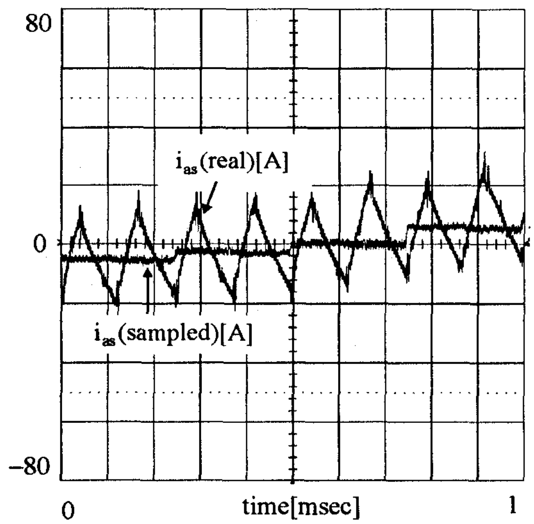

Fig. 7. Real current and sampled current with delayed sampling (experiment)

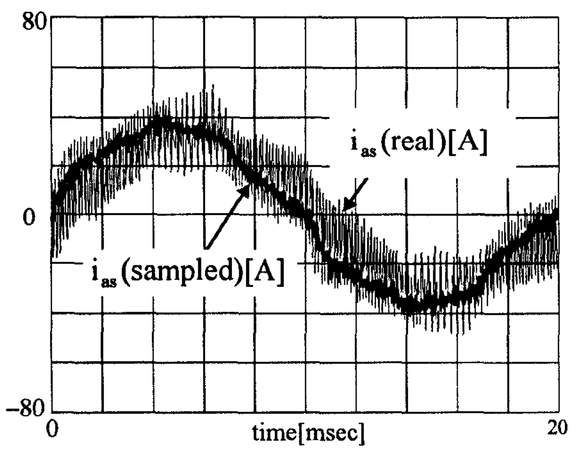

(a) without delayed sampling

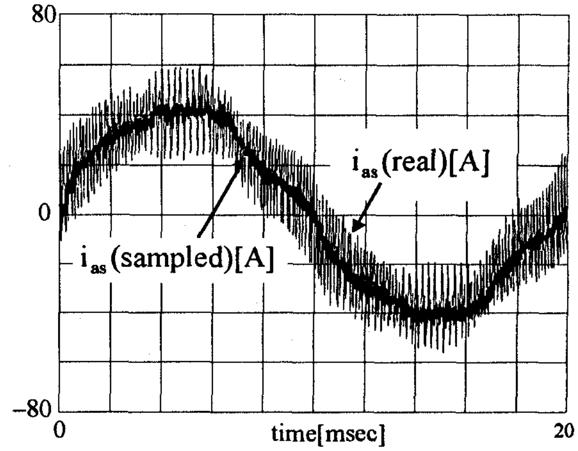

(b) with delayed sampling

Fig. 8. Real current and sampled current without and with delayed sampling (experiment : bold line indicates sampled current)

As shown in Fig. 5(a) and Fig. 8(a), there are current phase and magnitude error without delayed sampling. These result in a torque regulation failure and the simulation result for this is shown in Fig. 9. In Fig. 9, the average value of generated torque is less than the reference torque. On the other hand, the average value of generated torque is nearly same as reference torque with delayed sampling, which is shown in Fig. 10.

IV. Conclusion

In this paper, the antialiasing filter and its effect on current regulation was considered. The filter can be removed without aliasing effect by considering PWM strategy. The effect of a low pass filter to suppress switching noise was investigated and it has been proposed that the magnitude and phase error from the noise cut-off filter can be avoided with delayed sampling. The effect of the delayed sampling was verified with some experimental waveforms.

Appendix

A. Motor

11 kW induction motor for spindle application.
4 pole, Base speed 1500 rpm, Maximum speed 6000 rpm.
Rs=0.04Ω, Rr=0.0175Ω
Ls=6.6mH, Lr=6.6mH, Lm=6.45 mH.

B. Inverter

DC Link Voltage 370 V,
IGBT PWM inverter,
Space Vector 3 phase Symmetry PWM,
Switching Frequency 4 kHz,
Sampling Frequency 8kHz.

C. Current Regulator

Back-emf compensated PI regulator on synchronously rotating reference frame. Fully digital 8 kHz sampling.

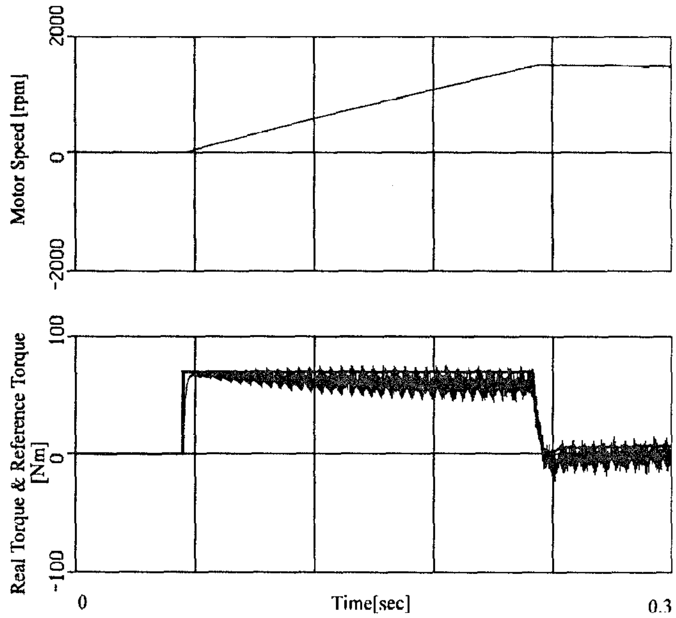

Fig. 9. Real torque and reference torque without delayed sampling (simulation)

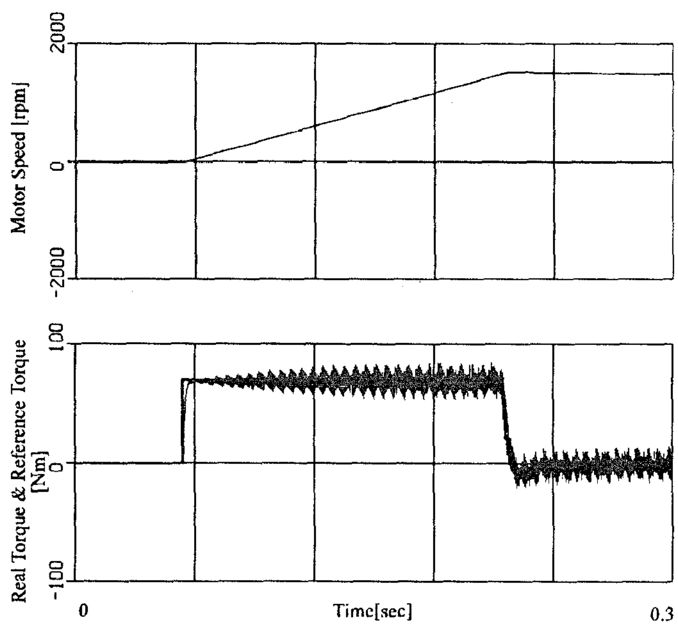

Fig. 10. Real torque and reference torque with delayed sampling (simulation)

Reference

[1] David M. Brod and Donald W. Novotny, "Current Control of VSI-PWM Inverters," *IEEE Trans. on Ind. Appl.*, vol. IA-21, no. 4, May/June, pp.562~570, 1985.

[2] Timothy M. Rowan and Russel J. Kerkman, "A New Synchronous Current Regulator and an Analysis of Current-Regulated PWM Inverters," *IEEE Trans. on Ind. Appl.*, vol. IA-22, no. 4, July/Aug., pp.678~690, 1986.

[3] G. Pfaff, A. Weschta and A. F. Wick, "Design and Experimental Results of a Brushless AC Servo Drive," *IEEE Trans. on Ind. Appl.*, vol. IA-20, no. 4, July/Aug., pp.814~821, 1984.

[4] L. Ben-Brahim and A. Kawamura, "Digital Current Regulation of Field-Oriented Controlled Induction Motor Based on Predictive Flux Observer," *IEEE IAS Conf. Rec.*, pp.607~612, 1990.

[5] Robert D. Lorenz and Donald B. Lawson, "Performance of Feedforward Current Regulators for Field-Oriented Induction Machine Controllers," *IEEE Trans. on Ind. Appl.*, vol. IA-23, no. 4, July/Aug., pp.597~602, 1987.

[6] Dong-Choon Lee, Seung-Ki Sul and Min-Ho Park, "High Performance Current Regulator for a Field-Oriented Controlled Induction Motor Drive," *IEEE Trans. on Ind. Appl.*, vol. IA-30, no. 7, Sep./Oct., pp.1247~1257, 1994.

[7] Jong-Woo Choi, Heui-Wook Kim and Seung-Ki Sul, "New Current Control Concept-Minimum Time Current Control in Induction Machine Drive," *IEEE IECON Conf. Rec.*, pp. 311~316, 1995.

[8] Raymond B. Sepe and Jeffrey H. Lang, "Implementation of Discrete-Time Field-Oriented Current Control," *IEEE Trans. Ind. Appl*, vol. 30, no 3, May/June 1994, pp. 723-727.

[9] H. van der Broeck, "Analysis of the Harmonics in Voltage Fed Inverter Drives caused by PWM Schemes with Discontinuous Switching Operation," *Conf. Rec. of EPE'91* vol.3,1991, pp. 261-266.

[10] Dae-Woong Chung, Joohn-Sheok Kim and Seung-Ki Sul, "Unified Voltage Modulation Technique for Real Time Three-Phase Power Conversion," *IEEE-IAS Anual Meeting Conf. Rec.*, 1996, in press.